Uncertainty Evaluation Method for Axi-Symmetric Measurement Machines

Abstract: This paper describes a method of uncertainty evaluation for axi-symmetric measurement machines. Specialized measuring machines for the inspection of axisymmetric components enable the measurement of properties such as roundness (radial runout), axial runout and coning. These machines typically consist of a rotary table and a number of contact measurement probes located on slideways. Sources of uncertainty include the probe calibration process, probe repeatability, probe alignment, geometric errors in the rotary table, the dimensional stability of the structure holding the probes and form errors in the reference hemisphere which is used to calibrate the system. The generic method is described and an evaluation of an industrial machine is described as a worked example. Expanded uncertainties, at 95% confidence, were then calculated for the measurement of; radial runout (1.2 µm with a plunger probe or 1.7 µm with a lever probe); axial runout (1.2 µm with a plunger probe or 1.5 µm with a lever probe); and coning/swash (0.44 arc seconds with a plunger probe or 0.60 arc seconds with a lever probe).

Keywords: Axi-Symmetric Measurement / runout / axial runout / radial runout

1 INTRODUCTION

An axi-symmetric measurement machine is a specialized measuring machine for the inspection of axisymmetric components enabling the measurement of properties

such as roundness (radial runout), axial runout and coning. This type of machine is not a polar coordinate measurement machine and cannot measure absolute dimensions such as the diameter or the height of components. Instead relative displacements are measured as a nominally axi-symmetric part is rotated about its axis. These types of measurements are particularly useful in measurement assisted assembly (MAA) for the optimisation of tolerances within assembly stacks [1]. As such these machines have become elements of metrology enabled manufacturing systems and in this context performance characterisation will enable the realisation of the Light Controlled Factory [2].

This paper describes a generic method of uncertainty evaluation for axi-symmetric measurement machines and gives an example of how this was applied to a commercially available machine; the iMAP machine from RPI. This study relates to the calibration uncertainty rather than the uncertainty of subsequent measurements and is therefore a best case performance for the machine. A process is described for producing an uncertainty budget. This involves carrying out repeatability and stability tests, obtaining calibration certificates and performing some calculations. Separate tests are required for each type of probe and a slightly different uncertainty budget is calculated for each type of measurement; roundness (radial runout); axial runout; and coning. Where convenient tests which lump together a number of sources of uncertainty are carried out since a full error separation calibration is not the aim.

There has been considerable work done to determine the uncertainty of roundness measurements using a Cartesian coordinate measurement machine (CMM) [3-6].

There has also been interest in the uncertainty of more specialized axisymmetric measurement machines showing that the fitting algorithms contribute little to combined uncertainty while reference standards are a large contributor [7]. Work has also shown that the uncertainty of industrial measurement instruments can be improved using improved algorithms [8]. State of the art instruments have been able to demonstrate standard uncertainties at the nanometre level for object's around 100 mm in diameter [9, 10]. This paper presents a clear process and case study for the application of uncertainty evaluation to a state of the art industrial measurement machine for axisymmetric components.

The evaluation of uncertainty of measurement, and not simply repeatability and reproducibility, is central to the rapidly developing Geometric Product Specification (GPS) standards [11]. Measurements should always be accompanied by a quantitative indication of uncertainty [12, 13] which establishes a range of values within which there is confidence that the true value lies. All the factors affecting the measurement result must therefore be considered and their effect on the measurement result quantified. Typical factors affecting measurements include random variation in use (repeatability); differences in results from different conditions such as different operators (reproducibility); the uncertainty of the reference standard accumulated through the traceability route of unbroken calibrations back to the primary standard; environmental factors such as temperature; alignments and setup parameters; and rounding errors.

For each of these factors components of uncertainty are obtained. These can be classified into Type A and Type B uncertainties. Type A evaluations are carried out

using statistical analysis of a series of observations while Type B evaluations are obtained by other means. The components may also be classified as either *random* or *systematic*.

Whether Type A or Type B, random or systematic, all uncertainties are modelled as probability distributions and quantified variances. These are statistically combined to give a combined standard uncertainty [12, 13] and then expanded by a coverage factor to give bounds to the possible range of values within which the true value may lie, at a given confidence level.

In this paper the iterative Procedure for Uncertainty MAnagement (PUMA) approach to the evaluation of uncertainty is taken. This involves initially over estimating 'worst case' contributions to the overall uncertainty where accurate values are not readily available, calculating the combined uncertainty and then determining whether an acceptable level of uncertainty has been evaluated. Where the combined uncertainty is found to be too high attempts are made to reduce significant sources of uncertainty where possible and improved estimates for **significant** contributors are obtained. This process is iterated until an acceptable level of uncertainty is obtained or no further improvement is possible. Using this approach the purpose of the first iteration is to understand the process and in particular identify dominant sources of uncertainty; subsequent iterations are then focused on reducing the variation in and improving estimation of these dominant sources. The process is illustrated in Figure 1. The PUMA approach is a practical method suited to industrial use, for the most rigorous uncertainty evaluations a

Monte Carlo approach is increasingly being taken [14] but this makes iterations more difficult.

2 MEASUREMENT SYTEM

The particular arrangement of axi-symmetric measurement machine considered in this paper is illustrated in Figure 2. It consists of a rotary table and a number of contact measurement probes located on slideways. The probes allow small deviations in the part to be measured as it is rotated and the slideways allow the probes to be manually positioned at different locations on the component.

Two different types of probe may be used: a *plunger* type probe in which the probe moves linearly and a *lever* type probe in which the probe rotates about an axis. A plunger probe is aligned so that its axis of movement is normal to the part being measure i.e. its axis of movement should pass through the part's axis of rotational symmetry. Any alignment errors will then remain constant throughout the range of measurement for a plunger probe. A lever probe is aligned so that the line through its point of contact with the part and its axis of rotation is tangential to the part. An initial movement of the part will then result in a movement of the probe normal to the surface of the part but as the probe rotates there will be an increasingly large cosine error.

3 SOURCES OF UNCERTAINTY

The sources of uncertainty in the measurements can be classified under six categories; Probe Calibration using gauge calibrator; use of probe; alignment of probe to part; rotary table geometric errors; dimensional stability of structure; and reference hemisphere. Each of these is described in the sub-sections below.

3.1. PROBE CALIBRATION USING GAUGE CALIBRATOR

The probe is calibrated before use using a micrometer based gage calibrator. Since the probe is used to make measurements of the displacement of the artefact as it is rotated it is not necessary to establish a zero point accurately. The probe is moved through its normal range in a series of discrete displacements and its voltage output is recorded along with the reference measurement from the gage calibrator. A straight line is then fit to these data points to establish the sensitivity of the probe in V/mm.

Sources of uncertainty for this probe calibration are; the uncertainty of the gage calibrator; the repeatability of the calibration process; the fitting error; and the probe resolution. The calibrator uncertainty is the uncertainty taken from the calibrator's calibration certificate and includes the uncertainty accumulated along the traceability chain. The probe calibration repeatability is the random variation between different calibrations; this includes process repeatability such as probe alignment, human error, differences in torque applied with tightening the screw and other differences between different operators. The calibration process involves fitting a straight line to the observed values. The mean for all calibrations of the standard errors in the fit of the line will be used as the fitting error. The probe resolution is the resolution of the voltage reading from the probe; this results in an uncertainty which is half of the smallest increment.

3.2. USE OF PROBE

When the measurement machine is being used to measure the roundness or some other property it is the probe which will actually interface with the component being

measured and sense any displacement. The use of the probe results in uncertainties due to the probe resolution; probe reversal spikes; and probe repeatability. Probe resolution is the resolution of the voltage reading from the probe and results in an uncertainty which is half of the smallest increment. The probe reversal spike is a dynamic error which occurs when the probe's moving stylus tip changes its direction of motion. The probe repeatability is the effect of random variation in use, it is quantified through a repeatability study which closely mimics the actual conditions of measurement and lumps together other sources of repeatability uncertainty.

3.3. ALIGNMENT OF PROBE TO PART

Uncertainty in the alignment of the probe to the part being measured results in an uncertainty in the result of the measurement. There are two alignment errors which will be considered. When there is an angular offset between the probe’s axis of measurement and the nominal surface normal this will result in a cosine error.

When there is an offset between the probe's point of contact and the true center line of the circular artefact this will result in an off-centre error

If the probe is aligned normally to the nominal circular profile of the part then there will be no probe cosine error since a change in the part radius *dr* will result in an equal movement of the probe *dM*. When there is an angular offset between the probe’s axis of measurement and the nominal surface normal, this will result in a cosine error so that *dM* is no longer equal to *dr* as shown in Figure 3. The cosine error is then the difference between the actual change in radius and the measured

distance as shown below. Unlike off-centre error, cosine error is not a function of artefact radius. For the lever probe, the worst case angular offset can be up to 15 degrees which can increase the significance of its cosine error.

$$\cos\theta = \frac{dr}{dM}$$
$$E_c = \frac{dr}{\cos\theta} - dr \qquad (1)$$

Probe off-centre error, Figure 4, occurs when there is an offset between the probe's point of contact and the true center line of the circular artefact *dy*, this will result in an error. When the radius changes by dr the probe will measure a change of dM. There are 2 off-centre offset (relative to x and y-axis of the hemisphere center) and together it can have a diagonal z-value which is the resultant off-set. This error is more or less the same for both the probes – plunger and lever.

$$dM = dr \cdot \cos\theta \qquad (2)$$

The probe off-centre error is the difference between the actual change in radius *dr* and the measurement result *dM*.

$$E_c = dr\left(1 - \cos\theta\right) \qquad (3)$$

The angle θ is a function of the radius and the offset *dy*

$$\theta = \arcsin\left(\frac{dy}{r}\right) \qquad (4)$$

So the probe off-centre error can be stated as

$$E_c = dr\left(1 - \cos\left(\arcsin\left(\frac{dy}{r}\right)\right)\right) \qquad (5)$$

3.4. TABLE GEOMETRIC ERRORS

A number of geometric errors inherent in the operation of the rotary table used to rotate the part being measured will affect the measurement result. These are coning or ‘swash’; axial runout; radial runout; axial interaction on radial runout; and radial interaction on axial runout.

Coning or ‘Swash’ is the result of the axis of symmetry for the axi-symmetric component not being aligned to the axis of rotation for the rotary table of the machine. This causes an apparent eccentricity when the part is rotated which increases linearly with distance along the axis.

Axial runout is the vertical movement in the table as it is rotated due to the table’s mechanism. Radial runout is the radial movement of the table as it is rotated.

Because a hemisphere is used as the reference during the instrument calibration there is an interaction between the measurements of axial and radial runout. For example when measuring axial runout the probe is placed at the top of the hemisphere to measure any vertical movement. Radial runout will cause the hemisphere to move sideways and since the top surface is not flat this will result in an apparent vertical movement when monitoring the probe reading. This is illustrated in Figure 5.

Considering a horizontal movement of the reference hemisphere due to radial runout *dy*, the resulting displacement of the probe *Ea* and the hemisphere radius *r* forming a right angle triangle we can say that

$$dy^2 + (r - E_a)^2 = r^2 \qquad (6)$$

Rearranging this gives the error due to radial interaction on axial runout *Ea*

$$E_a = r - \sqrt{r^2 - dy^2} \qquad (7)$$

Axial interaction on radial runout and radial interaction on axial runout will have equal values and be the same regardless of the type of probe used.

3.5. DIMENSIONAL STABILITY OF STRUCTURE

The dimensional stability of the structure must be considered including any creep of clamped interfaces; vibration; elastic compression and thermal expansion.

Uncertainty due to thermal changes in the structure and also any sagging in the structure can be evaluated by monitoring probe deflection over a period of time equivalent to a typical measurement and during which maximum thermal variation is encountered. Typical thermal disturbances might include opening a door or exposing the instrument to direct sunlight.

Creep and vibration must be considered when carrying out a repeatability study. Elastic deformation may cause errors which repeat and are therefore not detected in a repeatability study. Some simple tests are required placing the probe on a non-rotating part of the structure and starting and stopping the table to see if deformations are seen.

3.6. REFERENCE HEMISPHERE

Form and position errors in the reference hemisphere used for calibration will affect the uncertainty of the process. The hemisphere roundness value is simply taken from the hemisphere's calibration certificate. The hemisphere centring error is the (horizontal) distance between the hemisphere centre and table centre. The machine uses a software algorithm which corrects for this error although some residual error may remain.

3.7. UNCERTAINTY BUDGET INPUT QUANTITIES

Slightly different uncertainty budgets are required for each type of measurement since uncertainty in the probe travel needs to be translated/converted into axial runout, radial runout and coning using different sensitivity coefficients. Each budget will however have the same sources of uncertainty which are listed below:

- Calibrator Instrument Uncertainty
- Probe calibration repeatability
- Probe Calibration Fitting Error
- Probe resolution (calibration)
- Calibrator resolution
- Probe resolution (in use)
- System repeatability
- Probe cosine error
- Probe off-center error
- Axial/Radial Runout Interaction

- Table Axial Runout
- Table Radial Runout
- Table Coning
- System Stability
- Elastic Deformation
- Hemisphere Roundness

4 UNCERTAINTY EVALUATION PROCEDURE

Considering the sources of uncertainty described above generic procedure was created to enable the uncertainty of axi-symmetric measurement machines to be evaluated in a consistent and valid way. This follows the sequence shown in Figure 6 with the values obtained at each stage being entered into a spreadsheet which is then used to calculate the combined uncertainty using an uncertainty budget with sensitivity coefficients derived from the equations above.

4.1. STEP 1: LOOK UP VALUES FOR TYPE B UNCERTAINTIES AND CRITICAL DIMENSIONS

The first step in the uncertainty evaluation is to obtain Type B uncertainty values, predominantly from calibration certificates, and critical dimensions. The following Type B uncertainties were identified:

- Probe calibrator instrument uncertainty
- Probe reading rounding error
- Probe calibrator rounding error
- Reference hemisphere peak and valley (roundness values)
- Reference hemisphere calibrations uncertainty

At this stage the radius of the reference artefact used in calibration must also be identified. Although this is not an uncertainty value it will affect the sensitivity coefficients for probe alignment errors according to equations (5) and (7). The values recorded are shown in Table 1, where these values are represented as variables in equations within the text the variables are also given.

4.2. STEP 2: ESTIMATE ALIGNMENT AND GEOMETRIC ERRORS

Initial worst case estimates for alignment and geometric errors, given in Table 2, were shown to have a negligible effect on the combined uncertainty. In the table where these values are represented as variables in equations within the text the variables are also given. It was therefore determined that worst case estimates were sufficient and accurate evaluation of these uncertainties was not attempted.

Using these estimates it is then possible to calculate; Off-Centre Error; Cosine Error for plunger probe; Cosine Error for lever probe; and Axial-Radial Runout Interaction. These values are calculated using equations (5), (1) and (7) respectively. The alignment and geometric errors calculated in this way are given in Table 3.

The off-centre error, the cosine error for the plunger probe and axial-radial runout interaction can all be considered negligible and therefore the worst case estimates used for the input quantities are sufficient. The cosine error for the lever probe does represent a significant uncertainty, in this case however the estimated angle relates to the operating procedure for the probe and can therefore be considered an accurate estimate. This source of uncertainty could be reduced by restricting the range of operation for the probe.

4.3. STEP 3: PROBE CALIBRATION REPEATABILITY STUDY

The probe calibration process is not perfectly repeatable and this leads to uncertainty when the probes are used, additionally the assumption of perfect linearity may lead to additional uncertainty. A repeatability study was carried out for each type of probe to determine both of these sources of uncertainty.

The calibration process involves moving the probe through a number of known displacements using the probe calibrator as a reference and recording the voltage output at each of these displacements. A line is then fitted through the data points and the coefficients of this line (V/mm) are recorded to characterise the probe for subsequent measurement. For a plunger probe a simple straight line fit is used and therefore a single sensitivity coefficient characterizes the probe. For the lever probe the response is non-linear and a 5^{th} Order polynomial is used.

In the repeatability study the calibration is carried out a number of times and the standard deviation in the gradient of the line at the zero point is calculated, this gives the repeatability of the probe calibration. The standard fitting error for the best fit line is also calculated for all trials giving the probe calibration fitting error. In this study 10 calibrations were carried out to determine the calibration repeatability.

The plunger probe is calibrated close to mid-region of the probe stylus travel where the voltage reading ranges from -1.500 V to +1.500 V giving a probe travel range of 0.60 mm. The effective range of the probe is 1 mm. The probe voltage of 0.000 is initially set as datum and then the probe is extended by 0.300 mm where the

voltage (of close to -1.500 V) is recorded before commencing the probe calibration process. The probe is then compressed by 0.600 mm, using a Mitoyo calibrator, at a consistent step size of 0.010 mm giving 61 data points. A perfect plunger probe would give reading from -1.500 to 1.500 at an increment of 0.050 V. A straight line was fitted to the obtained data points using a least squares regression method in order to obtain the sensitivity of the probe in V/mm, it is therefore not necessary to carry out each calibration over exactly the same mid-range.

In order to reduce the time taken for the probe calibration repeatability study a number of different step sizes were evaluated. This indicated that there was a negligible difference in the calculated sensitivity and standard fitting error when the step size was increased to 0.02 mm and therefore this increased step size was used for the repeatability study reducing the number of data points which were recorded to 31. Table 4 shows the calculated sensitivity and standard fitting error for each repetition. Based on these results the standard deviation in the sensitivity can be calculated to be 0.00112 V/mm. The mean standard error is 0.00074 V which is sufficiently small to show that any non-linearity in the probe has a negligible impact on overall uncertainty.

All of the calibration measurements are taken when the probe is being compressed against a load. When the probe is extended, the voltage readings are different from the ‘compressed’ values at the same probe position

The lever probe has non-linear behaviour since the stylus rotates about a pivot point. As for the plunger probe the voltage reading is given in the range from -0.584 to +0.377 V.

Similar to the plunger probe calibration process, the probe voltage of 0.000 is initially set as datum and then the probe is displaced from -0.300 mm to +0.300 mm to record the voltage at every step point. Again calibrations were carried out at different step sizes to determine an optimum step size which in this case was found to be 0.050 mm. In this case there is a non-linear relationship between the probe displacement and the voltage output with a 5^{th} order polynomial being fit by the Acuscan software. To enable a sensitivity coefficient to be calculated for use in the uncertainty budget this was linearized about the range +/-50 μm. Table 5 shows the calculated sensitivity for each repetition. Based on these results the standard deviation in the sensitivity can be calculated to be 2.58 mV/mm. The standard error in the fitted line is 0.15 mV which is sufficiently small to show that any non-linearity in the probe over the range of +/-50 μm has a negligible impact on overall uncertainty. Again the uncertainty sensitivity coefficients are calculated as the reciprocal of the mean of the probe sensitivities.

4.4. REPEATABILITY STUDY 2: REPEATABILITY OF THE MEASUREMENT PROCESS

For each type of measurement (radial runout, axial runout and coning) the reference sphere was measured 10 times. The mean of the resulting measurement was used as an estimate of the table geometric error and the standard deviation of the results as an estimate of the system repeatability.

The system repeatability is used to determine the geometric errors in the table; probe repeatability in use; structure vibration; residual hemisphere off-centring error; probe geometric errors; and probe reversal spikes. Before carrying out the repeatability study the machine is setup according to the following steps:

1) The rotary table was setup for measurement using both the reference hemisphere and calibrated probes. When aligning the probes, the voltage reading was set to within 5 microns of zero. It doesn't have to be exactly zero because the interest lies in relative motion rather than absolute.
2) 2 revolutions of the table were run to let the table system stabilize. The surface speed to remained constant throughout.

For each repetition in the repeatability study the following steps are carried out, at least 10 repetitions should be carried out:

1) The plunger was positioned at the side and the lever at the top of the hemisphere (this is position A)
2) The radial runout (using plunger) and axial runout (using lever) were measured over for 10 revolutions.
3) The probe positions were reversed (this is position B)
4) The radial runout (using lever) and axial runout (using plunger) were measured over 10 revolutions.
5) The hemisphere was raised by a height of 520 mm (position C) using a stand.
6) The radial runout was measured over 10 revolutions using both probes. The coning/swash value is calculated.

Table 6 shows the results of the repeatability study.

4.5. SYSTEM STABILITY TEST

A system stability test was carried out to determine the effects of thermal expansion on the machine structure, electrical creep in the probe reading and any other sources of drift due to environmental variation over the duration of the measurement process. The probe was placed against the artefact and the output from the probe was recorded over 3 minutes which is the normal duration of a measurement. While the test was being carried out various environmental disturbances were induced. A number of these tests were carried out with different types of environmental disturbance detailed below:

- Condition a: Start with warmed up (30 revs) machine and reasonable warm surrounding conditions using heaters at the start of the 3.5 minutes. Note the voltage reading. And then open a door to blow cold air (ideally in winter) and note the max & min values.
- Condition b - Start with cold machine early morning with 2 revs to stabilize the machine. Note the voltage reading. And then expose the machine to direct sunlight or increase temperature using heater and note the max & min values.
- Condition c – any environmental condition as per customer requirements.

The range of observed values for these conditions was used in the overall uncertainty budget which was 0.001 V.

5 UNCERTAINTY BUDGET

For each type of measurement and each probe an uncertainty budget was created. Each of these followed the general layout and structure of the uncertainty budget

for the measurement of radial runout using a plunger probe (Table 7) but the table geometric error is different for each type of measurement and the sensitivity coefficients used are dependent on both the type of measurement and the probe used. A list of sensitivity coefficients with reference to the equations used to calculate them is given in Table 8 where each sensitivity coefficient is used in each uncertainty budget as detailed in Table 7.

Both A and D come from the same source, the probe calibration, where a linear relationship is determined between known displacements of the probe and the output voltage of the probe. This process is explained in detail in section 3.1. The sensitivity coefficient A is used to convert uncertainties in the calibrated probe sensitivity, in V/mm, into a length dependent uncertainty in μm/ μm, the length dependency is based on the deflection of the probe. A_P is used for the plunger probe and A_L for the lever probe.

A_P = 0.2 mm/V, A_L = 0.96 mm/V

The sensitivity coefficient B is used to convert uncertainties in the probe measurement in μm into uncertainties in the measurement of coning in arc seconds.

$$B = \arctan\left(\frac{1}{H}\right) \cdot 3600 \text{ = 0.41 arc sec/ μm} \qquad (8)$$

where H is the height difference, in μm, between the two measurements of radial runout.

The sensitivity coefficient C is used to convert the calibrated probe sensitivity in V/mm into a length dependent uncertainty in the measured coning angle arc sec / μm, with the length dependency again based on the deflection of the probe.

$$C = A \cdot B \qquad (9)$$

C_P = 0.08 arc sec/V, C_L = 0.39 arc sec/V

The sensitivity coefficient D is to convert uncertainties in the probe output in V into uncertainties in the measurement of runout in μm.

D_P = 200 μm/V, D_L = 960 μm/V

The sensitivity coefficient E is used to convert uncertainties in the probe output in V into uncertainties in the measurement of coning in arc seconds.

$$E = D \cdot B \qquad (10)$$

E_P = 82 arc sec/V, E_L = 394 arc sec/V

The combined uncertainty is therefore given by

$$u_c^2 = A^2 \qquad (11)$$

6 CONCLUSIONS

A novel and generic uncertainty evaluation process was developed and has been demonstrated for an industrial axisymmetric measurement machine. The expanded uncertainties, at 95% confidence, were calculated for the measurement of; radial runout radial runout (1.2 μm with a plunger probe or 1.7 μm with a lever probe);

axial runout (1.2 µm with a plunger probe or 1.5 µm with a lever probe); and coning/swash (0.44 arc seconds with a plunger probe or 0.60 arc seconds with a lever probe). Consideration of the uncertainty budgets will enable further optimization of the machine's uncertainty by focusing on the dominant sources of uncertainty according the PUMA methodology.

Each source of uncertainty is shown as a percentage of the combined uncertainty in Figure 7 and Figure 8. It is clear that for measurements with a plunger probe the uncertainty is dominated by the calibrator uncertainty with the system repeatability and table geometric errors also of some significance for runout measurements. For measurements with a lever probe the calibrator uncertainty remains the most significant and the system repeatability and table geometric errors are now strong contributors. Two probe related sources are also very significant; the probe cosine error and the system stability.

It may be accepted that the lever probe is inherently less accurate than the plunger probe and for measurements requiring the highest accuracy a plunger probe should be used with an improved calibration process.

AKNOWLEDGEMENTS

The research described herein has been carried out as part of the EPSRC, Light Controlled Factory Project (grant No. EP/K018124/1) at the Laboratory for Integrated Metrology Applications (LIMA) in the Mechanical Engineering Department of the University of Bath. Thanks is given to the support and technical expertise from Rotary Precision Instruments, in particular Jim Palmer and Ian Whitehead.

REFERENCES

1. Mei, Z. and P.G. Maropoulos, *Review of the application of flexible, measurement-assisted assembly technology in aircraft manufacturing.* Proceedings of the Institution of Mechanical Engineers, Part B: Journal of Engineering Manufacture, 2014. **228**: p. 1185-1197. DOI: 10.1177/0954405413517387
2. Muelaner, J.E. and P.G. Maropoulos, *Large Volume Metrology Technologies for the Light Controlled Factory.* Procedia CIRP, 2014. **25**: p. 169-176
3. Gapinski, B. and M. Rucki. *Uncertainty in CMM measurement of roundness*. 2007. Trento, Italy: Inst. of Elec. and Elec. Eng. Computer Society.
4. Gapinski, B., L. Ocenasova, and M. Rucki. *Strategy of roundness measurement with CMM*. 2008. Trnava, Slovakia: Danube Adria Association for Automation and Manufacturing, DAAAM.
5. Gapinski, B. and M. Rucki. *Analysis of cmm accuracy in the measurement of roundness*. 2009. Haifa, Israel: ASME.
6. Ruffa, S., G.D. Panciani, F. Ricci, and G. Vicario, *Assessing measurement uncertainty in CMM measurements: Comparison of different approaches.* International Journal of Metrology and Quality Engineering, 2013. **4**(3): p. 163-168. DOI: 10.1051/ijmqe/2013057

7. Nielsen, H.S. and M.C. Malburg, *Traceability and correlation in roundness measurement.* Precision Engineering, 1996. **19**(2-3): p. 175-179. DOI: 10.1016/s0141-6359(96)00004-9

8. Mudronja, V., M. Katic, and V. imunovic. *Improvement of roundness measurement with Mahr MMQ3*. 2008. Cavtat-Dubrovnik, Croatia: Croatian Metrology Society.

9. Giardini, W.J. *High precision measurement of roundness and sphericity*. 1994. Adelaide, Aust: Publ by IE Aust.

10. Neugebauer, M., *Uncertainty analysis for roundness measurements by the example of measurements on a glass hemisphere.* Measurement Science and Technology, 2001. **12**(1): p. 68-76. DOI: 10.1088/0957-0233/12/1/309

11. Nielsen, H.S., *Recent developments in International Organization for Standardization geometrical product specification standards and strategic plans for future work.* Proceedings of the Institution of Mechanical Engineers, Part B: Journal of Engineering Manufacture, 2013. **227**: p. 643-649. DOI: 10.1177/0954405412466986

12. UKAS, *M3003 - The Expression of Uncertainty and Confidence in Measurement*. 2007, UKAS, Doc

13. BSI, *General Metrology - Part 3: Guide to the expression of uncertainty in measurement (GUM)*, in *PD 6461-3*. 1995.

14. Shen, Y., Y.L. Xin Luo, and X. Chen, *A Monte Carlo analysis of uncertainty in supporting assembly of large-aperture optical lenses.* Proceedings of the

Institution of Mechanical Engineers, Part B: Journal of Engineering Manufacture, 2013. **227**: p. 1504-1513. DOI: 10.1177/0954405413489293

15. ISO. *BS EN ISO 14253-2:2011 - Geometrical product specifications (GPS). Inspection by measurement of workpieces and measuring equipment. Guidance for the estimation of uncertainty in GPS measurement, in calibration of measuring equipment and in product verification*. 2011

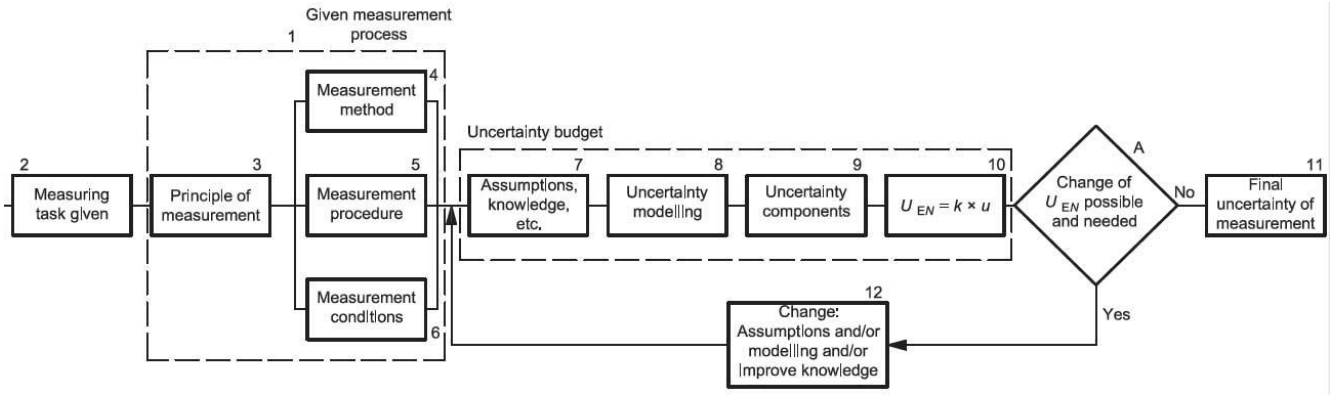

Figure 1 – The PUMA Method of Uncertainty Evaluation [15]

Figure 2 – An Axi-Symmetric Measurement Machine

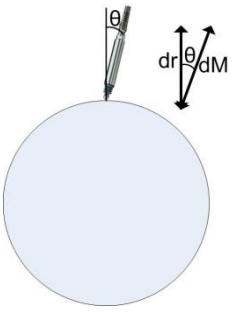

Figure 3 – Probe Cosine Error

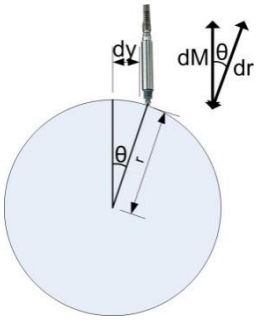

Figure 4 – Prove Off-Centre Error

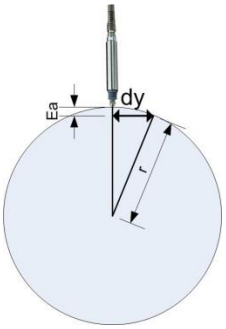

Figure 5 – Axial/Radial Runout Interaction

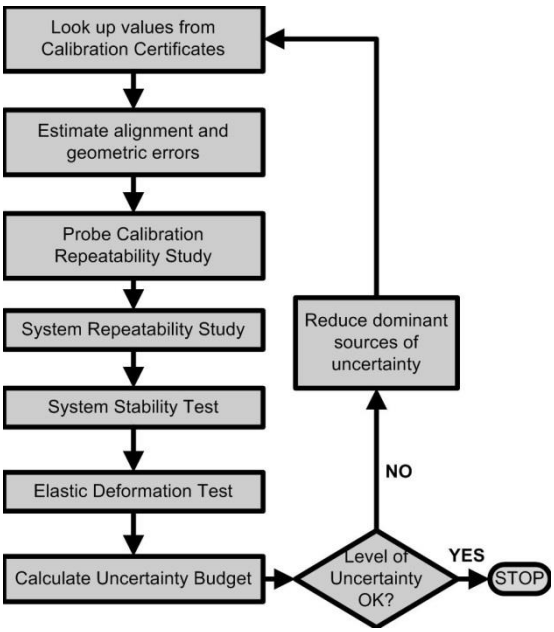

Figure 6 – Uncertainty Evaluation Process

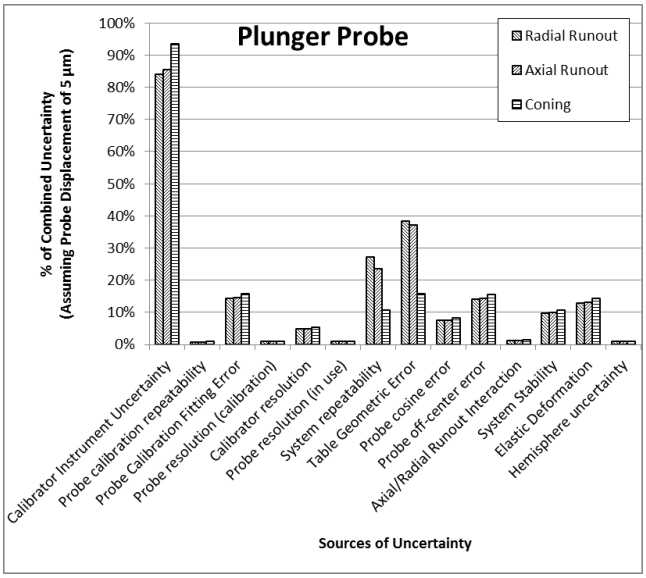

Figure 7 – Contributions of Uncertainty Sources for Measurements with a Plunger Probe

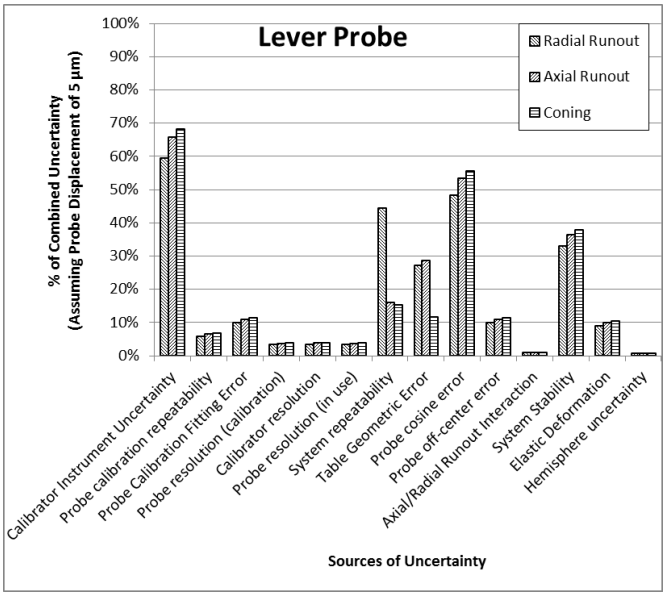

Figure 8: Contributions of Uncertainty Sources for Measurements with a Lever Probe

Table 1 – Values Recorded in Step 1

Source	Variable	Value
Probe Calibrator Instrument Uncertainty (k=1 value)		1 µm
Smallest Increment of probe reading (2x resolution uncertainty)		0.0001 V
Smallest Increment on probe calibrator (2x resolution uncertainty)		0.1 µm
Reference Hemisphere radius	***r***	25 mm
Reference Hemisphere component peak		0.004 µm
Reference Hemisphere component valley		-0.004 µm
Reference Hemisphere Calibration Uncertainty		0.006 µm

Table 2 – Values Estimated in Step 2

Source	Variable	Value
Offset of probe from component centre-line	***dy_c***	3 mm
Change in component radius	***dr***	10 µm
Eccentricity		10 µm
Angular offset (cosine error) for plunger probe	***θ***	5°
Angular offset (cosine error) for lever probe	***θ***	15°
Perpendicular Movement (radial runout when measuring axial etc)	***dy_l***	25 µm

Table 3 – Calculated Alignment and Geometric Errors

Source	Value
Off-Centre Error	0.14452 µm
Cosine Error for plunger probe	0.0764 µm
Cosine Error for lever probe	0.70552 µm
Axial-Radial Runout Interaction	0.0125 µm

Table 4: Results of Plunger Probe Calibration Repeatability Study

Trial	Best fit Sensitivity (V/mm)	Standard Error In Gradient (V)
1	5.00471	0.00054
2	5.00247	0.00086
3	5.00174	0.00081
4	5.00191	0.00073
5	5.00397	0.00057
6	5.00171	0.00079
7	5.00300	0.00071
8	5.00272	0.00092
9	5.00232	0.00074
10	5.00453	0.00068

Table 5: Results of Lever Probe Calibration Repeatability Study

Trial	**Best fit Sensitivity (V/mm)**
1	1.040
2	1.045
3	1.045
4	1.045
5	1.040
6	1.040
7	1.040
8	1.040
9	1.040
10	1.045

Table 6 – Results of Repeatability Study

Probe	Measurement	Table Geometric Errors	System Repeatability
Plunger	Radial Runout	0.40 µm	0.16 µm
	Axial Runout	0.38 µm	0.14 µm
	Coning	0.15 arc sec	0.06 arc sec
Lever	Radial Runout	0.40 µm	0.37 µm
	Axial Runout	0.38 µm	0.12 µm
	Coning	0.15 arc sec	0.11 arc sec

Table 7 – Uncertainty Budget for the Measurement of Radial Runout using a Plunger Probe

Source of Uncertainty	Absolute Value	Relative values	Distribution	Divisor	Sensitivity Coefficient	Absolute Standard Uncertainty (µm)	Relative Standard Uncertainty (µm/µm)
Calibrator Instrument Uncertainty	1 µm		Normal	2	1	0.500	
Probe calibration repeatability		0.00112 V/mm	Normal	1	0.2 mm/V		0.0002
Probe Calibration Fitting Error	0.000735 V		Rectangular	1.7321	200 µm/V	0.085	
Probe resolution (calibration)	0.00005 V		Rectangular	1.7321	200 µm/V	0.006	
Calibrator resolution	0.05 µm		Rectangular	1.7321	1	0.029	
Probe resolution (in use)	0.00005 V		Rectangular	1.7321	200 µm/V	0.006	
System repeatability	0.16 µm		Normal	1	1	0.162	
Table Radial Runout	0.40 µm		Rectangular	1.7321	1	0.228	
Probe cosine error	0.076 µm		Rectangular	1.7321	1	0.044	
Probe off-centre error	0.145 µm		Rectangular	1.7321	1	0.083	
Axial/Radial Runout Interaction	0.013 µm		Rectangular	1.7321	1	0.007	
System Stability	0.0005 V		Rectangular	1.7321	200 µm/V	0.058	
Elastic Deformation	0.00038 V		Normal	1	200 µm/V	0.076	
Hemisphere uncertainty	0.01 µm		Rectangular	1.7321	1	0.006	
					Combined Standard Uncertainty	**0.595**	**0.000**
					Expanded Uncertainty (k=2)	**1.191**	**0.000**

Table 8 – Sensitivity Coefficients used in Uncertainty Budgets

Source of Uncertainty	**Radial Runout (Plunger Probe)**	**Axial Runout (Plunger Probe)**	**Coning (Plunger Probe)**	**Radial Runout (Lever Probe)**	**Axial Runout (Lever Probe)**	**Coning (Lever Probe)**
Calibrator Instrument Uncertainty	1	1	B	1	1	B
Probe calibration repeatability	A_P	A_P	C_P	A_L	A_L	C_L
Probe Calibration Fitting Error	D_P	D_P	E_P	D_L	D_L	E_L
Probe resolution (calibration)	D_P	D_P	E_P	D_L	D_L	E_L
Calibrator resolution	1	1	B	1	1	B
Probe resolution (in use)	D_P	D_P	E_P	D_L	D_L	E_L
System repeatability	1	1	B	1	1	B
Table Radial Runout	1	1	B	1	1	B
Probe cosine error	1	1	B	1	1	B
Probe off-centre error	1	1	B	1	1	B
Axial/Radial Runout Interaction	1	1	B	1	1	B
System Stability	D_P	D_P	E_P	D_L	D_L	E_L
Elastic Deformation	D_P	D_P	E_P	D_P	D_P	E_P
Hemisphere uncertainty	1	1	B	1	1	B